Check for updates

Leaf wax biomarkers of a high-mountain lake area in western iberia—Implications for environmental reconstructions

Ricardo N. Santos[1,2,3]*, Enno Schefuß[4],
Lívia Gebara M. S. Cordeiro[2,3], Dulce Oliveira[2,3],
Armand Hernández[5], Alexandre M. Ramos[1,6] and
Teresa Rodrigues[2,3]*

[1]IDL—Instituto Dom Luiz, Faculty of Sciences of the University of Lisbon, Lisbon, Portugal,
[2]IPMA—Portuguese Institute for the Sea and Atmosphere, Lisbon, Portugal, [3]CCMAR—Algarve Centre
of Marine Sciences, Algarve University, Faro, Portugal, [4]MARUM—Center for Marine Environmental
Sciences, University of Bremen, Bremen, Germany, [5]CICA—Centre for Advanced Scientific Research,
University of Coruña, GRICA Group, A Coruña, Spain, [6]Institute of Meteorology and Climate Research,
Karlsruhe Institute of Technology, Karlsruhe, Germany

Leaf wax *n*-alkane biomarkers are widely used to infer past vegetation dynamics
and hydroclimate changes. The use of these compounds strongly relies on the
characterization of modern plants. However, few studies have explored leaf
waxes of modern plants and their application to reconstructing climate and
environmental changes in the Iberian Peninsula, a region known for its high
vulnerability to climate change. In this study, we characterize the distributions
and compound-specific isotopic compositions of the leaf waxes of dominant
plants in the vegetation cover, soil, and surface sediment of the Lake Peixão
area, a high-mountain glacial lake in Serra da Estrela (central Portugal). Our
results show that the modern oro-Mediterranean (subalpine) vegetation of the
study area is dominated by C_3 grasses/herbs and shrubs that preferentially
produce long-chain leaf waxes ($\geq C_{27}$). The C_{31} *n*-alkane display the overall
highest concentration, produced by some grasses and shrubs, but especially
Erica sp (heather), which is highlighted as a major source for the total *n*-alkane
pool in the lake sediments. C_{29} is the second-most abundant and the most
equally produced *n*-alkane of the vegetation cover; C_{25} and C_{27} homologs are
mainly associated with aquatic-related grasses/herbs, while C_{33} and C_{35} are
particularly linked to cold-drought tolerant *Juniperus* sp. shrubs. Shrubs show
higher but proportional values than grasses/herbs in the isotopic space,
suggesting a directly proportional physiological adaptation of the two
ecological forms to the prevailing climatic and environmental factors of the
study area. C_{29} is pointed as the most representative (or less plant-biased) leaf
wax *n*-alkane in the lake sediments. Thus, δD of C_{29} *n*-alkane is interpreted as a
robust terrestrial hydrological indicator (δD$_{terr}$), which signal is believed to be
strongly influenced by the mean air temperature and/or precipitation amount.
Despite the sparse vegetation and small catchment area, the apparent hydrogen
fractionation factor, determined from δD$_{terr}$ of the lake surface sediment, is in
line with the modeled global mean values for the latitude of the study area. The
different molecular and compound-specific signatures of the studied

oro-Mediterranean species have the potential to support future interpretations of leaf wax biomarkers in the Iberian Peninsula.

GRAPHICAL ABSTRACT
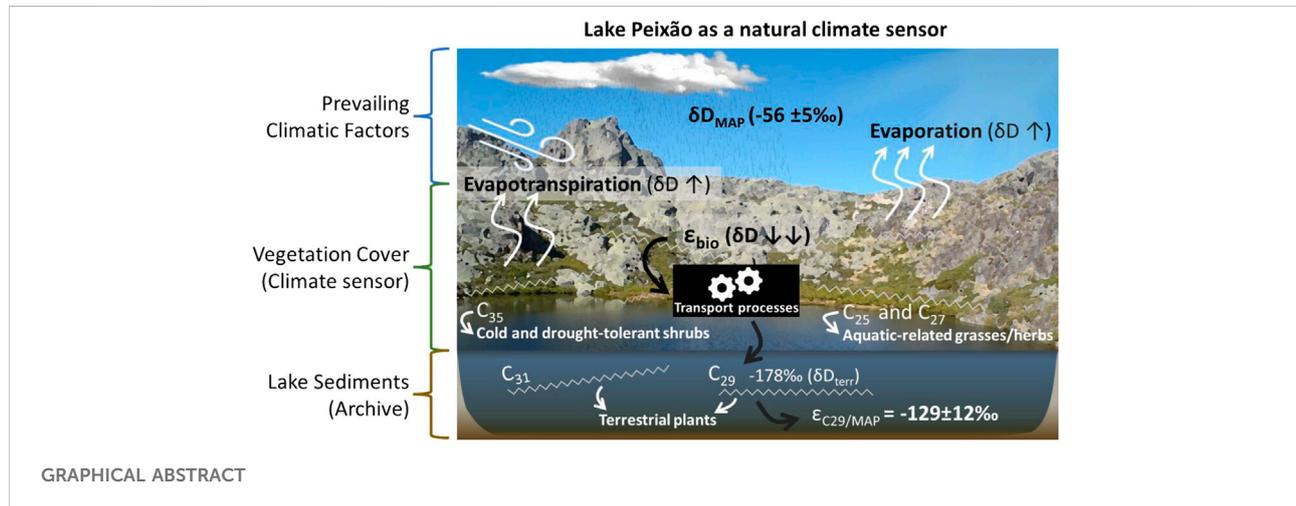
1 Introduction

Reconstruction of past climate and environmental conditions requires a thorough characterization and understanding of how modern ecosystems produce physical, chemical, or biological indicators, known as proxies, in response to specific climatic and environmental conditions. An ecosystem that promptly responds to climate change is often referred to as a "climatic sensor" (Evans et al., 2013). An excellent example of this type of sensor is the vegetation cover of the Iberian high mountains, known as sensitive ecosystems and natural laboratories (Toro et al., 2006). The lakes of these high mountains can act as sentinels of climate and environment changes and are capable of archiving evidence of the temporal evolution of the surrounding landscape in their sediments (Adrian et al., 2009). The Iberian Peninsula (IP) displays a wide range of climatic conditions due to its mid-latitude location, between the Eastern North Atlantic and the western Mediterranean regions, its complex orography, and the interplay between sub-tropical and sub-polar air masses. These features make IP bioclimatic diverse and particularly sensitive to climate changes and a recognized "hot spot" for the study of past climate, especially in quaternary studies (e.g., Sánchez-López et al., 2016; Abrantes et al., 2017; Baldini et al., 2019; Thatcher et al., 2020).
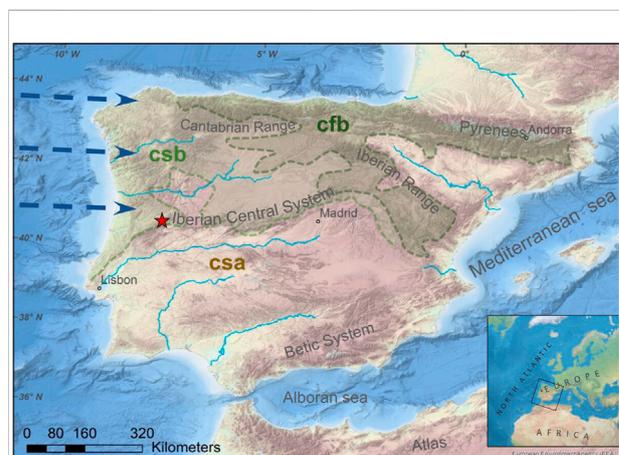
FIGURE 1

Morphological map of the Iberian Peninsula. The red star indicates the Lake Peixão location (Serra da Estrela, Portugal). Csa: Hot summer Mediterranean climate; Csb: Mild summer Mediterranean climate; Cfb: Oceanic. The dark blue arrows represent the moist rich prevailing westerlies from the Atlantic Ocean entering Iberia. Sources: European map from shadedrelief.com. River network from the European Environment Agency (EEA). Topography and bathymetry, sourced from portal.emodnet-bathymetry.eu, overlapped with the simplified Köppen-Geiger climate classification for the Iberian Peninsula (1971–2000) (adapted from the Iberian Climate Atlas, 2011).
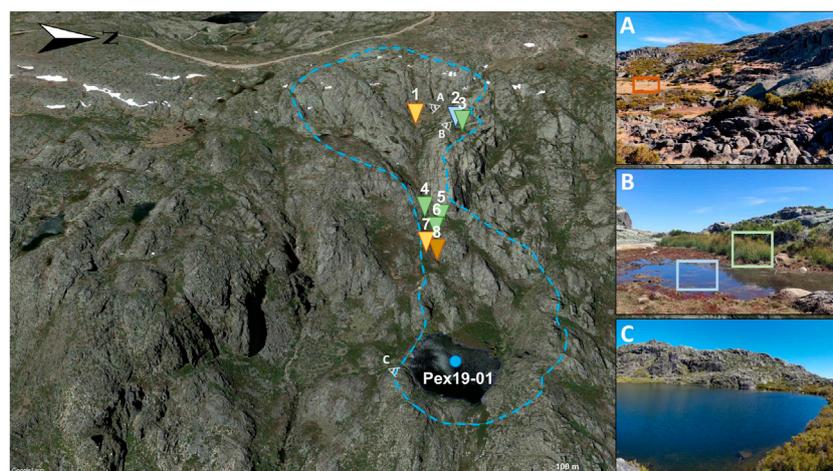
FIGURE 2
The Lake Peixão area. The light-blue dashed line represents the upslope watershed contour obtained from the elevation model of Google Earth Pro. The enumerated triangles represent sites of sample collection: 1—*Agrostis* sp.; 2—*Antinoria* sp.; 3—*Juncus* sp.; 4—*Cytisus* sp.; 5—*Juniperus* sp. and respective litter; 6—*Erica* sp. and respective litter; 7—*Nardus* sp. and respective litter; 8—Soil sample. Colors represent orange—grasses; light blue—aquatic grass; light green—soft rush; dark green—shrub; brown—soil. The eye-view symbol point to the view seen in the respective photos **(A,B)**, and **(C)**. Satellite imagery from Google Earth (date: 26 May 2019).

Plants produce a wide range of organic compounds, including leaf wax biomarkers, which are used as climate and environmental proxies (Peters et al., 2005; Castañeda and Schouten, 2011; Berke, 2018). However, the use of these compounds requires a comprehensive characterization of modern plants composition and understanding of their respond to the prevailing climate and environment factors (e.g., Bush and McInerney, 2013; Howard et al., 2018; Liu et al., 2018; Wang et al., 2018). The characterization of modern leaf wax compositions in the IP is still understudied (Ferreira et al., 2007; Ortiz et al., 2010, 2011, 2016; López-Días et al., 2013), despite the increasing number of past reconstructions using these compounds in both marine and lacustrine records (e.g., Jambrina-Enríquez et al., 2016; Taylor et al., 2018; Schirrmacher et al., 2020; Toney et al., 2020). Here, we focus on leaf wax n-alkanes, n-alkyl lipids with the general formula of C_nH_{2n+2} (where n is the carbon number in the chemical chain), synthesized by plants to act as a protective barrier from the external environment and prevent water loss (Eglinton and Hamilton, 1967; Cranwell et al., 1987; Post-Beittenmiller, 1996; Shepherd and Griffiths, 2006). The high resistance to degradation and strong isotopic relationship of n-alkanes with vegetation type and water sources make compound-specific stable isotope analysis (CSIA) a valuable tool to infer past organic matter sources and hydrologic changes (e.g., Leider et al., 2013; Curtin et al., 2019; Hahn et al., 2021; Imfeld et al., 2022). Temporal variations in the stable carbon isotope ratio ($^{13}C/^{12}C$) of n-alkanes ($\delta^{13}C_{n\text{-alk}}$) in sedimentary records generally reflect changes in vegetation sources and water use efficiency of a catchment area (e.g., Freeman and Colarusso, 2001; Schefuß et al., 2003; Rommerskirchen et al., 2006; Diefendorf and

Freimuth, 2017). The hydrogen isotopic ratios (D/H) of leaf wax n-alkanes ($\delta D_{n\text{-alk}}$) ultimately reflect the isotopic composition of precipitation. However, this signal results from a net fractionation process involving isotopic signatures of groundwater, lake water, soil, plant transpiration, and biosynthetic fractionation (see Sachse et al., 2012 for review).

In this work, we aim to fill the gap in studies of modern plants and their relationship as precursors of hydrocarbon biomarkers in IP. For that, we explored leaf wax n-alkanes of predominant species in the vegetation cover and surface sediment of Lake Peixão. This study area, located on top of the Serra da Estrela Mountain, lies between the Atlantic and Mediterranean bioclimatic zones, being considered a sensitive place to explore past hydrological changes and is in one of the most vulnerable regions to current climate changes (Allan et al., 2021). These results will add new insights about leaf wax biomarkers in IP and ultimately contribute to more reliable and robust interpretations of their sedimentary records in this key-region for reconstructing past climate and environmental changes.

2 Materials and methods

2.1 Study area

The study area is located in the Serra da Estrela Mountain, a NE–SW-directed intraplate mountain range in the westernmost sector of the Iberian Central System (Figure 1), central Portugal. This alpine range of the granitic basement (Ribeiro et al., 1990)

comprises the highest point (1,993 m above mean sea level, amsl) and the largest nature conservation area of continental Portugal. Here, a remarkable and unique set of glacial landforms and deposits (e.g., see Vieira, 2004, 2008) promoted the recognition of this region as a UNESCO Global Geopark. One of these glacial features is the study site, Lake Peixão (Figure 1) (40°20′35″N; 7°36′19″W), a relatively small (0.015 km^2) and subcircular lake (ca. 140 m diameter) at 1,677 m amsl. This alpine lake has a glacial origin, formed after the melting of the last icesheets ca. 14.7 ± 0.32 ka cal BP, which the small catchment area (ca. 0.30 km^2) is characterized by enclosed and steep granitic rocks (Figure 2) [Hernández et al., (2022) (in review)]. Few and small ephemeral streams flow into the lake, which has slightly acidic, oligotrophic, and monomitic waters (Boavida and Gliwicz, 1996). A spill point in the southern part can control the maximum lake level, draining into the Candeira valley (Figure 2). The landscape near the lake is characterized by sparse but well-constrained oro-Mediterranean vegetation patches dominated by shrubs such as *Erica* spp., *Juniperus communis*, *Genista* spp., *Cytisus* spp., and *Calluna vulgaris* (Connor et al., 2021), and grasslands mainly composed by *Agrostis delicatula* and *Nardus stricta*. Soils are rare and poorly developed; aquatic plants are sparse and mainly located near ponds and the lake, while trees are absent.

In general, Serra da Estrela region is characterized by a Mediterranean climate, with warm/dry summers and cold/wet winters, and is marked by strong vertical gradients in temperature and precipitation (Vieira et al., 2005; Mora, 2010). The ensemble historical climate of the region, from 1971 to 2000 [see http://portaldoclima.pt/en (Accessed 29 March 2022)], shows that the warmest and driest months are July and August, with mean values of approximately 20°C and 17 mm of rainfall. The coldest and wettest months are December and January, with a mean temperature of approximately 5°C and 150 mm precipitation, where precipitation often falls in the form of snow on the top of the mountain (Carreira et al., 2009, 2011).

The spatial variability of precipitation in this mountain range is highly controlled by altitude and slope orientation, with the basal areas receiving approximately half of the precipitation amount of the mountain summit, which can reach values of approximately 2,500 mm/year (Mora, 2010). The mountain range roughly defines a boundary between two Mediterranean climates (following the Köppen–Geiger climate classification system), one to the north characterized by mild summers (csb) and the other to the south characterized by hot and dry summers (csa) (Figure 1). The moisture-rich westerlies are predominant during winters and show a gradual D-depletion from the coast inland (Carreira et al., 2009). The atmospheric moisture sources of this part of the IP are almost exclusively derived from the prevailing westerly Atlantic air masses (Carreira et al., 2009; Cortesi et al., 2013; Thatcher et al., 2020), contrasting with other regions, such as the southeastern, which can also be significantly influenced by Mediterranean sources (Cortesi et al., 2013; Taylor et al., 2018; Schirrmacher et al., 2020; Toney et al.,

2020). The high-altitude setting of Serra da Estrela results in temperature being an important driver of moisture condensation and the δD value of precipitation (δD$_{prc}$) (Carreira et al., 2009; Oliveira and Lima, 2010). This is reflected by a strong relationship between mean values of δ^{18}O and δD vs. temperature of monthly rainfall for Portugal's mainland (Carreira et al., 2009), which is also observed in other Iberian mountains (Giménez et al., 2021). The combination of the settings mentioned above and climatic and environmental factors makes Serra da Estrela one of the most biodiverse in Europe (Jansen, 2011) and a prime location to investigate the relationship between climate and ecology (Connor et al., 2021).

2.2 Material

A total of seven samples of dominant vegetation (four grass/herbs and three shrubs), three vegetation litters (one grass/herbs and two shrubs), a soil sample collected from the Lake Peixão catchment area (Figure 2), and a lake surface sediment. Modern plant samples were collected in September 2020; each plant sample was composed of several branches or leaves from different plants near the same collecting spot. These samples were wrapped in aluminum foil and sealed in an airtight bag. The vegetation litter samples were collected beneath the respective plant to ensure their source, and the soil sample comprises the top 2 cm of one of the few places in the lake's catchment where soils were available (Figure 2). Both litter and soil samples were collected directly with precombusted jar glasses. All samples were stored in a cool bag, directly transported to the Portuguese Institute of Sea and Atmosphere (IPMA, Portugal), and stored in a cool room (~5°C) until analysis. The lake surface sediment sample correspond to the 0 cm–1 cm depth of 8.63 m long core retrieved from the center of the Lake Peixão in June 2019 (PEX19-01) using a UWITEC® Piston Corer. Based on ^{210}Pb measurements, this surface sediment sample comprises 11 ± 4 years [Hernández et al. (2022) in review].

2.3 *n*-alkane analyses and characterization

All samples were freeze-dried, homogenized, and analyzed in the Biogeochemistry laboratory at IPMA. The vegetation samples were composed of leaves and stems from seven samples. Depending on the vegetation type, wood and stems were removed as much as possible. The samples were cut into small pieces with clean metal scissors. The three samples of the vegetation litter, the soil sample, and the lake surface sediment sample presented minimal clastic material (silt and clays), and no sieving was needed. Before extraction, 1,000 ng of an internal standard solution (hexatriacontane, tetracontane, and

nonadecanol-1-ol) was added to approximately 2.5 g of the sample. The lipid compounds were extracted three times using dichloromethane in an ultrasonic bath.

The total lipid extract (TLE) was hydrolyzed with potassium hydroxide in methanol (KOH/MeOH 6%, ~12 h, at room temperature). The neutral fraction containing *n*-alkanes was recovered with *n*-hexane by liquid–liquid extraction and cleaned with ultrapure water to remove traces of KOH. The *n*-alkanes were fractionated from the neutral extracts using 5 cm of deactivated silica gel (0.040 μm–0.063 μm mesh) and AgNO₃-silica gel Pasteur pipette columns with *n*-hexane as eluent. The *n*-alkane extracts were dried and diluted with toluene, and 1 μl was injected into a gas chromatography-flame ionization detector (GC-FID; Varian Model 3,800) equipped with a 1,079 programmable temperature vaporizing injector (PTV) for cold on-column with a CPSIL-5 CB column coated with 100% dimethylsiloxane capillary column (50 m × 0.32 mm × 0.12 μm film coating) connected to a fused silica precolumn (5 m × 0.25 mm × 0.25 μm). The oven temperature was programmed from 90° (holding time of 1 min) to 170°C at 20°C/min, then to 280°C at 6°C/min (holding time 25 min), and finally, to 315°C at 10°C/min (holding time of 12 min). The injector was programmed from 90°C (holding time of 0.5 min) to 310°C at 200°C/min. Samples were injected (1 μl) in split mode using H₂ as the carrier gas (~2.5 ml/min). The temperature of the detector was constant at 320°C with 35 ml/min of H₂ flow, 300 ml/min of airflow, and 30 ml/min of N₂ flow. The total run time for each sample was 63.83 min.

The *n*-alkanes were identified by comparing the retention times to an external standard mixture (*n*-alkanes ranging from C₁₇-C₃₆). The *n*-alkane concentrations (ng/g, dry weight sample) were determined based on the internal standard *n*-hexatriacontane (C₃₆).

Several indices have been developed to characterize the *n*-alkane distributions of samples (see Li et al., 2020). The most widely used are (a) the average chain length (ACL, Poynter, 1989); (b) the carbon preference index (CPI, Bray and Evans, 1961; Marzi et al., 1993), and (c) the proportion of aquatic plants (P_aq, Ficken et al., 2000).

(a) The ACL is used to identify the preferentially produced *n*-alkane length chains in a sample (Poynter, 1989) based on a weighted average of the *n*-alkane concentrations from C₂₇ to C₃₃, calculated as:

$$ACL_{27-33} = odd\sum_{n=27}^{33}(Cn \times n)\Big/\sum_{n=27}^{33}(Cn) \qquad (1)$$

where C_n is the concentration of a given *n*-alkane and *n is* the number of carbons in its chain.

(b) The CPI is the concentration weighted ratio of odd to even *n*-alkane chain lengths, which is normally used to examine the general source of sedimentary biomarkers and/or degradation processes. It can be calculated as follows:

$$CPI_{27-33} = 1\Big/2[odd\sum_{n=27}^{33}(Cn)\Big/even\sum_{n=26}^{32}(Cn)$$
$$+ (odd\sum_{n=27}^{33}(Cn)\Big/even\sum_{n=28}^{34}(Cn)] \qquad (2)$$

where C_n is the concentration of a given *n*-alkane.

(c) The P_aq commonly used to evaluate the relative contributions of *n*-alkanes from aquatic versus terrestrial plants in the lake sediments: $P_{aq}=(C_{23} + C_{25})/(C_{23} + C_{25} + C_{29} + C_{31})$, where C_{23} and C_{25} are considered from aquatic-related plant origins, whereas C_{29} and C_{31} are from terrestrial plants (Ficken et al., 2000).

CSIA was conducted on the *n*-alkanes when amounts were allowed by gas chromatography-isotope ratio mass spectrometry (GC-IRMS) at the MARUM Center for Marine Environmental Science, University of Bremen (Germany).

The $\delta^{13}C_{n\text{-alk}}$ values were measured with a Thermo Trace GC Ultra coupled to a Finnigan MAT 252 mass spectrometer. The *n*-alkane extracts were injected in splitless mode before being oxidized to CO_2 by a combustion reactor at 1,000°C. The instrument was equipped with an HP-5ms capillary column (30 m × 0.25 mm × 0.25 μm film coating); helium was the carrier gas (purity 99.999%) at a constant flow of 1.5 ml/min. The produced CO_2 was then injected into the mass spectrometer for analysis. The injector temperature was programmed to be constant at 250°C. The GC temperature was set from 120°C (hold time of 3 min) to 320°C at a heating rate of 5°C/min (hold time of 15 min). The $\delta^{13}C_{n\text{-alk}}$ values of the individual compounds were calibrated by injecting pulses of CO_2 from an external reference gas that was automatically introduced into IRMS at the beginning and end of each analysis. The $\delta^{13}C$ values are reported in ‰ relative to the Vienna Pee Dee Belemnite (VPDB) standard and represent an average of duplicates with a standard deviation less than 0.5‰ whenever *n*-alkane amounts allowed for multiple runs.

Standard $\delta D_{n\text{-alk}}$ was performed on a Thermo Trace GC equipped with an HP-5ms column (30 m × 0.25 mm × 0.10 μm film coating) coupled to a Thermo Fisher MAT 253 (IRMS) *via* a pyrolysis reactor (operated at 1,420°C). The GC oven program was similar to the conditions used to analyze the carbon isotopic composition. The injection of known isotopic composition standards after every six measurements and the daily determination of the H^{3+} factor using H_2 reference gas were used to control measurement accuracy. The $\delta D_{n\text{-alk}}$ was calibrated against an external H_2 reference gas and reported

TABLE 1 – *n*-Alkane concentrations* and indices (ACL$_{27-33}$, CPI$_{27-33}$, P$_{aq}$) of plant leaves and stems and soil and surface sediment samples from the Lake Peixão (Serra da Estrela, Portugal).

Sample	Ecological form	Environment	(*n*-alkanes ng/g)																			(*n*-alkanes ng/g)	*n*-alkane indices		
			Sample type**	C$_{17}$	C$_{18}$	C$_{19}$	C$_{20}$	C$_{21}$	C$_{22}$	C$_{23}$	C$_{24}$	C$_{25}$	C$_{26}$	C$_{27}$	C$_{28}$	C$_{29}$	C$_{30}$	C$_{31}$	C$_{32}$	C$_{33}$	C$_{34}$	C$_{35}$	Total *n*-alk***	ACL$_{27-33}$	CPI$_{27-33}$	P$_{aq}$
Agrostis sp.	grass/herb	terrestrial	Veg	11	326	65	193	354	145	2,857	1912	45,038	4,765	96,331	15,640	**130,298**	9,927	112,330	5,719	15,198	833	563	4.43 × 10^5	29.3	10.4	0.2
Nardus sp.	grass/herb	terrestrial	Veg	155	286	5	200	39	102	910	948	14,346	3,420	19,565	8,361	106,318	7,281	**307,444**	4,367	56,622	184	1,332	5.32 × 10^{5}	30.6	22.6	0.0
Antinoria sp.	grass/herb	aquatic-related	Veg	128	266	159	250	1,523	1,163	5,795	4,868	**33,311**	2,985	18,591	2074	16,629	1,349	25,081	1,054	22,256	186	1703	1.39 × 10^5	30.2	14.4	0.5
Juncus sp.	grass/herb	aquatic-related	Veg	28	218	263	89	830	690	3,685	1,222	2,905	1892	**12,554**	1,040	5,212	239	2,775	203	300	78	168	3.44 × 10^4	28.1	9.8	0.5
Erica sp.	shrub	terrestrial	Veg	45	204	188	201	4,360	1,018	6,152	1,411	12,809	3,831	84,604	13,728	311,759	42,497	**659,377**	41,027	178,062	2,669	845	1.36 × 10^6	30.5	12.3	0.0
Juniperus sp.	shrub	terrestrial	Veg	5	7	0	33	4	78	275	103	413	171	1,225	453	6,556	1,196	33,999	15,430	**373,934**	23,653	88,742	5.46 × 10^5	32.8	17.2	0.0
Cytisus sp.	shrub	terrestrial	Veg	4	322	32	206	255	681	**39,449**	3,532	24,616	757	6,830	756	13,283	1,447	18,675	369	538	55	80	1.12 × 10^5	29.7	13.4	0.7
Nardus sp. (L.)	grass/herb	terrestrial	Veg. litter	28	63	2	30	43	56	100	58	253	50	504	160	3,635	430	**17,934**	579	7,780	113	402	3.22 × 10^4	31.2	23.9	0.0
Erica sp. (L.)	shrub	terrestrial	Veg. litter	61	134	8	59	50	48	95	67	207	65	590	142	2,365	365	**11,105**	690	5,552	86	137	2.18 × 10^4	31.2	15.4	0.0
Juniperus sp. (L.)	shrub	terrestrial	Veg. litter	25	156	0	61	318	113	430	80	664	153	2,755	519	10,323	1870	37,055	6,652	**118,922**	3,845	15,050	1.99 × 10^5	32.2	15.8	0.0
Soil sample	-	terrestrial	soil	1	3	8	5	27	29	57	19	105	30	312	81	1,117	103	**1,561**	124	790	33	46	4.45 × 10^3	30.5	11.2	0.1
Lake surface sediment	-	lake	sediment	392	421	1,161	695	2,968	1,504	5,482	2,702	8,899	4,231	15,116	3,975	22,677	3,251	**37,111**	3,069	19,609	841	1921	1.36 × 10^5	30.3	7.5	0.2

*Highest concentrations values in bold; **Veg. meaning vegetation; ***sum of *n*-alkane concentrations from C$_{17}$ to C$_{35}$.
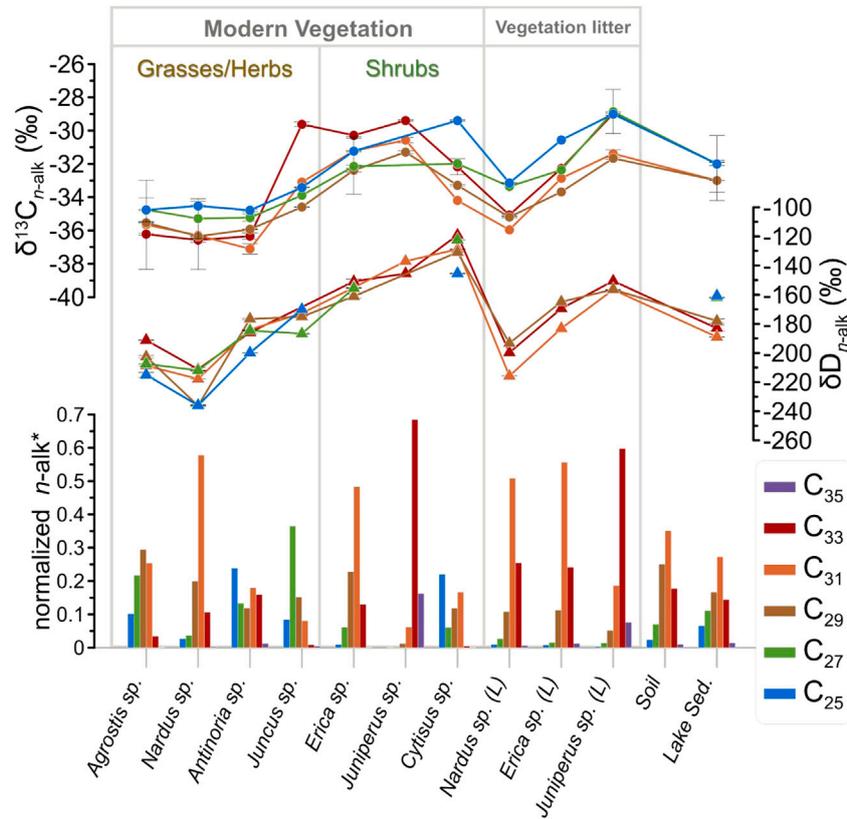
FIGURE 3
n-alkane distributions and compound-specific isotopic values (C_{25}—C_{35}) of the dominant plants, vegetation litter (L.), soil and surface sediment samples of the Lake Peixão area. The whiskers correspond to 1 SD, where multiple measurements on the respective compound were performed. *Normalization against the total n-alkane concentration of each sample.
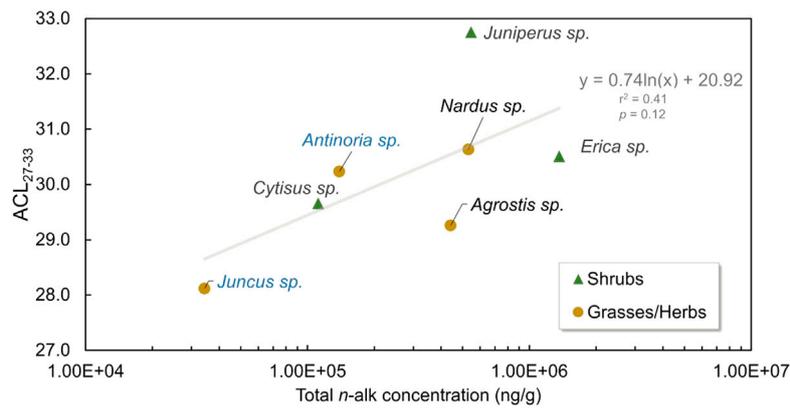

FIGURE 4
ACL_{27-33} vs. total n-alkane concentrations (ng/g, in logarithmic scale) of the two dominant ecological forms of the Lake Peixão catchment. The overall trend is represented by a logarithm regression line in gray. Green triangles represent shrubs; colored circles represent grasses/herbs, aquatic-related plants in blue, and nonaquatic plants in yellowish.

FIGURE 5
ACL$_{27-33}$ vs. δ^{13}C of C$_{29}$ n-alkane in modern plants of the Lake Peixão area. Blue names correspond to aquatic-related grasses, and yellowish names correspond to nonaquatic-related grasses/herbs plants.
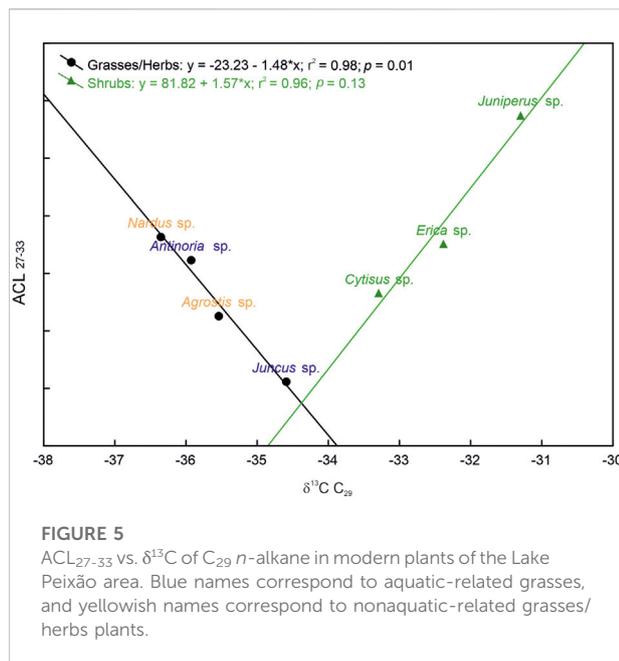
in ‰ Vienna Standard Mean Ocean Water (VSMOW). When n-alkane amounts allowed multiple runs, the samples were run in duplicate, and the reported values represent the mean with a standard deviation less than 3‰.

The apparent fractionation (ε$_{app}$) between δD of leaf wax n-alkanes (δD$_{n-alk}$) and precipitation (δD$_{prc}$) was calculated using the equation described in Sessions et al. (1999): ε$_{n-alk/water}$ = 1,000 [(δD$_{n-alk}$+1,000)/(δD$_{prc}$+1,000)] −1, in ‰. The δD$_{prc}$ used as a reference for the mean annual precipitation was estimated using the Online Isotopes in Precipitation Calculator (OIPC3.1; Bowen and Revenaugh, 2003) by constraining the central altitude, longitude, and elevation of the lake catchment area. This modeled δD$_{prc}$ value was then compared with the hydrogen isotopic value of nearby spring water.

3 Results

3.1 Distribution and concentration of n-alkanes

The modern vegetation samples exhibit the typical strong odd over even chain length predominance, with a wide range of total n-alkane concentration (sum of concentrations from C$_{17}$ to C$_{35}$ n-alkane), varying from 3.4×10^4 to 1.4×10^6 ng/g (dry weight) (Table 1). Most of the analyzed plants show a predominance of long-chain n-alkanes (≥C$_{27}$), particularly C$_{31}$ and C$_{29}$ homologs (Figure 3).

Principal component analysis (PCA) of the n-alkanes (concentration and isotopic compositions) performed in

PAST4.07 free software (Hammer et al., 2001) (Supplementary Figure S1) suggests that samples can be grouped according to the ecological forms: grasses/herbs and shrubs (see Figure 3). On the other hand, for ACL$_{27-33}$ (U, $p = 0.12$) and CPI$_{27-33}$ (U, $p = 0.35$) the Mann-Whitney U tests, performed in STATISTICA 7.0, suggests no statistical difference in between the two forms (Supplementary Figure S2). In addition, grasses/herbs and shrubs appear to share a generally positive trend between ACL$_{27-33}$ and total n-alkane concentration, however under low statistical significance (Figure 4). *Nardus* sp. and *Agrostis* sp. presented the highest n-alkane concentrations in this ecological form, preferentially producing C$_{31}$ and C$_{29}$, respectively (Table 1). *Antinoria* sp (aquatic-related grass) exhibits proportional amounts of C$_{25}$, C$_{31}$, C$_{33}$, and C$_{27}$ homologs (decrescent in this order) (Figure 3). *Juncus* sp (herb) has the lowest total n-alkane concentration and a maximum at C$_{27}$. *Erica* sp. is highlighted as having the highest total n-alkane concentration of among all the studied plants (Table 1). These species preferentially produce C$_{31}$, twenty times more than the other investigated shrubs. On the other hand, *Cytisus* sp. is the shrub with the lowest total n-alkane concentration but produces considerably more mid-chains than the other shrubs, particularly the C$_{23}$ homolog (Figure 3; Table 1).

The decrease in n-alkane concentration from vegetation to the respective litter samples was significant, although the dominant homolog is preserved from its vegetation source (Table 1). For example, *Juniperus* sp. displays a decrease of 68% in the dominant homolog (C$_{33}$), *Nardus* sp. a decrease of 96% in C$_{31}$, while *Erica* sp. a decrease of 97% in C$_{31}$. The soil sample exhibits a strong odd over even chain length dominated by long-chain n-alkanes, resulting in ACL$_{27-33}$ and CPI$_{27-33}$ values of 30.5 and 11.2, respectively (Table 1). The total concentration of odd C$_{27}$—C$_{33}$ chains is 3.8×10^3 ng/g (dry weight) and accounts for ~85% of the total n-alkane concentration. The lake surface sediment and soil samples share the same dominance and long-chain n-alkane distribution (Table 1) (C$_{31}$ > C$_{29}$ > C$_{33}$ > C$_{27}$ > C$_{25}$ > C$_{35}$) and similar ACL$_{27-33}$ (30.3). However, the lake sediments have a considerably larger concentration (thirty times more) of n-alkanes, lower CPI$_{27-33}$ (7.5), and higher P$_{aq}$ (0.19) than the soil sample (Table 1).

3.2 Compound-specific δ^{13}C$_{n-alk}$ (odd C$_{25}$—C$_{33}$)

The δ^{13}C$_{n-alk}$ values of the dominant plants of the Lake Peixão catchment area show an overall range of −37 to −29‰ (Supplementary Table S1), with minor differences between homologs but considerable interspecific variability (Figure 3). In general, longer carbon chains show the lowest δ^{13}C values, mainly C$_{29}$ and C$_{31}$ homologs (Figure 3). Grasses/herbs

display the most negative $\delta^{13}C$ values, ranging from −37 to −30‰. From those, *Juncus* sp. showed the highest values (−35 to −30‰) (Supplementary Table S1). The $\delta^{13}C_{n\text{-alk}}$ of shrubs varies from −34 to −29‰. *Juniperus* sp. and *Erica* sp. exhibit particularly narrow $\delta^{13}C$ ranges, the latter ranging from −32 to −30‰, whereas *Cytisus* sp. has a broader range (−34 to −29‰) (Supplementary Table S1). The $\delta^{13}C$ values of C_{29} in the two dominant ecological forms in the study area showed clear and opposite linear relationships with $ACL_{27\text{-}33}$ (Figure 5) and CPI (Supplementary Figure S3). The $\delta^{13}C_{n\text{-alk}}$ values of vegetation litter vary from −35 to −30‰, generally displaying similar values to their respective vegetation sources (Supplementary Table S1). The lake surface sediment shows similar $\delta^{13}C_{n\text{-alk}}$ values among homologs (−33 to −32‰), with the lowest values of C_{29} and C_{31} (Figure 3).

3.3 Compound-specific $\delta D_{n\text{-alk}}$ (odd C_{25}—C_{33})

The $\delta D_{n\text{-alk}}$ of the analyzed vegetation shows a wide range of values, from −236 to −119‰, with, grasses displaying lower $\delta D_{n\text{-alk}}$ values than shrubs (Supplementary Table S1). There is a remarkable difference between nonaquatic and aquatic-related grasses/herbs, with the latter showing higher $\delta D_{n\text{-alk}}$ values than their terrestrial counterparts. For example, for C_{27}, the terrestrial grasses *Agrostis* sp. and *Nardus* sp. display values of ca. −210‰, while *Antinoria* sp. and *Juncus* sp. show values of ca. -180‰ (Figure 3). In addition, *Cytisus* sp. showed higher and more variable values among homologs (−146 to −119‰) than plants such as *Erica* sp (−161 to −151‰) (Figure 3). Litter of Nardus sp. exhibits higher $\delta D_{n\text{-alk}}$ values than its source; in C_{29}, this relative increase corresponds to ca. 18%, from −236 to −193‰. This contrasts with shrub litter, which shows lower values than their sources (Figure 3). The δD values of C_{31} in *Erica* sp. represent a decrease of 18%, from −155 to −183‰, and in *Juniperus* sp., a similar decrease from −137 to −157‰ (Figure 3; Supplementary Table S1). The $\delta D_{n\text{-alk}}$ from lake surface sediment displays values ranging from −189 to −161‰, with C_{25} and C_{27} homologs showing the highest (similar) values (Figure 3). In contrast, longer chains, particularly C_{31}, displayed the lowest values.

3.4 Apparent hydrogen isotope fractionation

The modern δD of the mean annual precipitation (δD_{MAP}) estimated using OIPC3.1 for the study area is −56 ± 5‰, a value similar to the −53‰ mean value for the wetter months during the main growing season (from March to May) and within the range of the near-annual mean value of −51 ± 2‰ from the Fonte dos Perús spring, which is ca. 1 km of the study area but in the opposite façade of the mountain (Carvalho, 2013).
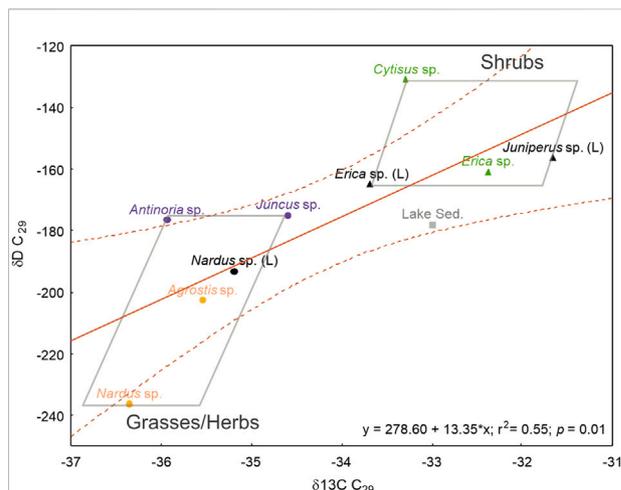

FIGURE 6
Isotopic space ($\delta^{13}C$ and δD values) of C_{29} *n*-alkane in the analyzed samples from the Lake Peixão area. Circles correspond to samples form grass/herb ecological forms, where blue circles relate to aquatic-related plants and yellowish circles relate to nonaquatic-related plants; triangles correspond to samples from shrub ecological forms (L) indicating litter sample from the respective plant. Lake Sed. (black square) corresponds to the surface lake sediment sample.

The specific fractionation factors ($\epsilon_{n\text{-alk/MAP}}$) determined for the modern vegetation range from −191 ± 17‰ to −67 ± 6‰ (Table 1) values constrained by a common δD_{MAP} value of the study area; error is given by the standard deviation of measurements in *n*-alkanes and δD_{MAP}. Therefore, *Agrostis* sp. and *Nardus* sp. display mean ϵ_{app} values (from C_{25} to C_{33}) of −158 ± 32‰ and −177 ± 35‰, respectively, whereas the aquatic-related counterparts, *Antinoria* sp. and *Juncus* sp., show higher values of −138 ± 28‰ and −127 ± 23‰, respectively. C_{31} was the only compound present in sufficient quantities in all three shrub species for reliable $\delta^{13}C/\delta D$ measurements; thus, using this component as a reference, *Erica* sp. shows the highest fractionation ($\epsilon_{C31/MAP}$ = −105 ± 9‰), while *Cytisus* sp. the lowest ($\epsilon_{C31/MAP}$ = −77 ± 7‰). The surface sediment of the lake also shows an increase in $\epsilon_{n\text{-alk/MAP}}$ from C_{29} > C_{33} > C_{31}, ranging from −129 ± 12‰ to −141 ± 13‰, and C_{25} and C_{27} homologs display the lowest $\epsilon_{n\text{-alk/MAP}}$, approximately −112 ± 10‰.

4 Discussion

4.1 Leaf wax *n*-alkane biomarkers of modern plants

The small and well-constrained catchment area of the Lake Peixão presents ideal characteristics for assessing the vegetation cover inputs into lake sediments. The C_{31} and C_{29} are the predominant *n*-alkanes of the modern plants in the vegetation

cover. Grasses/herbs and shrubs display similar ACL_{27-33} and CPI_{27-33} values (Supplementary Figure S2) that can suggest traits of a common physiological adaptation of this vegetation type, but also that the application of such indicators alone may be questionable to differentiate between the two terrestrial forms. This common physiological response may also be reflected in the suggested positive trend between ACL_{27-33} and n-alkane concentration (Figure 4); however, the limited dataset appears to constraint the statistical significance of this hypothesis, which will be likely addressed in future studies.

The high amount of n-alkanes produced by *Erica* sp. suggests that these plants are significant sources of leaf waxes in the study area, particularly the C_{31} n-alkane. These findings agree with other modern vegetation studies in the IP (Ferreira et al., 2007; Ortiz et al., 2016), where C_{31} n-alkane is pointed out as a possible indicator of heather inputs (Loidi et al., 2007; Ortiz et al., 2016). Our results also suggest that *Juniperus* sp. is another important source of long-chain n-alkanes ($\geq C_{33}$), accounting almost exclusively for the production of C_{35} in the vegetation cover (Figure 3; Table 1). These observations align with the results obtained for other species of *Juniperus* sp. in central Spain (Schäfer et al., 2016a), suggesting that these especially long-chains compounds can be used as an ecological proxy and indicators of arid and cold conditions (Thomas et al., 2007; Dasgupta et al., 2022). In Iberian heathlands, the relative increase in grasses/herbs over shrubs can reflect an increase in water availability, as they are often in contact with mires (Loidi et al., 2007). In the study area, the aquatic-related plants are restricted to the grass/herb ecological form, such as *Antinoria* sp. and *Juncus* sp., which are relatively abundant in small ponds and streams. The n-alkane analyses of these species suggest C_{27} and C_{25} as indicators of aquatic or aquatic-related plants matter and water availability in the lake Peixão ecosystem.

The relatively high contribution of mid-chain compounds of some shrubs, such as Cytisus sp., (Figure 3; Table 1), highlights that caution is needed when applying distributions n-alkane, such as P_{aq}, to infer past aquatic inputs or lake levels in downcore paleoreconstructions (Xie et al., 2020). However, the relative deviation in the n-alkane distribution of Cytisus sp. relative to other shrubs is not reflected in the isotopic space ($\delta^{13}C_{n\text{-alk}}$ and $\delta D_{n\text{-alk}}$) (Figures 3, 6), which encourages the application of CSIA to better assess vegetation sources in lake sediments. In fact, the two ecological forms are well-separated in the isotopic space (Figure 6), where the observed linear proportionality may result from the inferred common physiological response to the shared climatic and environmental conditions of the study area, i.e., precipitation, temperature, humidity, and water source. For example, the lower $\delta D_{n\text{-alk}}$ of grasses/herbs may imply lower transpiration rates and lower water loss than shrubs, but on the other hand, its lower $\delta^{13}C_{n\text{-alk}}$ values may also imply that grasses/herbs have less water use efficiency than shrubs (Hou et al., 2007; Gao et al., 2014). While the similar ACL_{27-33}/CPI_{27-33}, along with the proportionally distinct isotopic

values, are inferred to be the reason for the opposite trends between the two ecological forms in ACL/CPI vs. $\delta^{13}C_{n\text{-alk}}$ (e.g., Figure 5; Supplementary Figure S3).

4.2 The source of Lake Peixão n-alkanes and its implications for paleo-reconstructions

The strong predominance of odd-over-even carbon chain compounds, high ACL_{27-33}, and low P_{aq} values (Table 1) in the surface sediment of Lake Peixão suggests that the n-alkanes were primarily derived from terrestrial plants from the catchment area. Additionally the high CPI_{27-33} values (> 5) in the lake sediments suggest good preservation of the n-alkane content which gives confidence in the use of leaf waxes record in the lake sediments (Pancost and Boot, 2004).

Our results show that from plants to vegetation litter, and lake surface sediment the isotopic signal is well preserved despite important changes in n-alkane concentrations (Table 1). Moreover, the relative proportion of dominant chains (Figure 3) is also maintained The ACL_{27-33} and n-alkane distribution of modern soil and the lake surface sediment remain identical even though the latter reflects higher contribution of aquatic or aquatic-related plants (Figure 3; Table 1). On the other hand, the CPI_{27-33} offset between plants, vegetation litter, and the lake surface sediment reflects the complex plant-to-sediment transfer processes, which involve a series of admixtures of different plant inputs and biodegradation; for instance, by microbes (Zech et al., 2010; Schäfer et al., 2016b; Stout, 2020; Thomas et al., 2021).

The $\delta^{13}C_{n\text{-alk}}$ values (ca. $-33\permil$) of lake surface sediment suggest a predominance of C_3 plants (Figure 3) and reinforce shrubs as a major source of waxes in the study area (Figure 3; Table 1). The two dominant ecological forms produce significant and relatively equivalent amounts of C_{29}, showing proportional values of carbon and hydrogen fractionation that may result from a consistent physiological response of plants to the same environment and climatic factors. Thus, we expect C_{29} to provide a more holistic overview of the n-alkane composition of the terrestrial vegetation cover in the Lake Peixão sediments compared with other long-chain compounds, such as C_{31}, that appear to be particularly biased towards species like *Erica*. This hypothesis supports global compilations that report C_{29} as a widely produced terrestrial n-alkane strongly and consistently associated with regional mean δD_{prc} (Sachse et al., 2012; Liu and Liu, 2019; McFarlin et al., 2019). Moreover, the modern $\varepsilon C_{29}/_{MAP}$ value ($-129 \pm 12\permil$) of lake surface sediment is remarkably consistent with the global modeled values by Liu and An (2019) and McFarlin et al. (2019) for the latitude of the study area. Therefore, we suggest the δD of C_{29} as a robust indicator of terrestrial hydrology, i.e., δD_{terr}, in paleostudies in both sediments of Lake Peixão and downstream areas.

The strong relationship between temperature and precipitation is an important paleo-hydrological factor in the study area since plants mostly synthesize their n-alkanes during early growing season or when water is available (Freimuth et al., 2017; Diefendorf et al., 2021), which in the IP occurs during spring-early summer and the during autumn-winter (Pérez Latorre and Cabezudo, 2002; García-Alix et al., 2021). Therefore, the downcore temporal variability in the values of δD_{terr} in the Lake Peixão sediments is expected to mainly reflect bi-seasonal to annual changes in mean air temperature and/or precipitation amount. In the study site, lower temperatures often imply an increase in condensation, resulting in an inherent coupled effect of precipitation amount (amount effect) that may be imprinted in the δD_{terr}. Hence, low (high) δD_{terr} values in downcore reconstructions are expected to reflect a decrease (increase) in temperatures and/or increase (decrease) in precipitation (snow or rainfall).

Moreover, based on the ecology of modern plants and the compositions of different n-alkanes analyzed, we expected the δD values of C_{25} and C_{27} in the lake sediments to better reflect changes in lake water sources. The scarcity of true aquatic plants in the study area makes it challenging to confirm this hypothesis. Aquatic plants typically show higher $\delta^{13}C_{n\text{-alk}}$ values than their terrestrial counterparts (e.g., Jiménez-Moreno et al., 2013; Hockun et al., 2016; Ortiz et al., 2021), which is not evident in the lake surface sediment nor in the analyzed plants, only *Juncus* sp. displaying relatively higher $\delta^{13}C_{n\text{-alk}}$ than their ecological counterparts (Figure 3; Table 1). The lack of evidence of less $\delta^{13}C$ depletion in mid-chains n-alkanes in the lake surface sediment supports terrestrial plant dominance over aquatic plant inputs in modern lake settings. This suggests that caution needs to be taken when using mid-chain n-alkanes without compound-specific $\delta^{13}C$ analyses in sedimentary archives to infer past changes in aquatic plant inputs and lake waters (Hockun et al., 2016; McFarlin et al., 2019). Moreover, it also highlights the importance of using $\delta^{13}C_{n\text{-alk}}$ over other indicators, such as P_{aq}, to better constrain aquatic inputs in the lake sediments. Beyond that, the distinct values of ε_{app} between modern plants and lake surface sediment underline the importance of constraining the vegetation source when using specific fractionation factors in sediments (Yang et al., 2011).

5 Conclusion

Our results show that the oro-Mediterranean vegetation cover of the Lake Peixão area preferentially produces long-chain n-alkanes ($\geq C_{27}$) that control the n-alkane content in the lake. This vegetation is dominated by C_3 grasses/herbs and shrubs, two ecological forms that display similar $ACL_{27\text{-}33}$ and $CPI_{27\text{-}33}$ values but are clearly distinguished by their

n-alkane isotopic signatures. Shrubs show proportionally higher $\delta^{13}C_{n\text{-alk}}$ and $\delta D_{n\text{-alk}}$ values than grasses/herbs, suggesting a congruent physiological response to the common climatic and environmental conditions. The n-alkane C_{31} is the predominant leaf wax of the study area, produced by some grasses and shrubs, particularly by *Erica* sp. (heather), a shrub that is stands out as a major source for the total n-alkane pool. The C_{29} is the second-most abundant and the more equally produced leaf n-alkane of the two dominant ecological forms. The n-alkanes C_{33} and C_{35}, although less abundant than other long chains homologs, are also important in the study area since they are particularly associated with cold and drought-tolerant vegetation such as *Juniperus* sp. Finally, C_{27} and C_{25} n-alkanes are mainly linked to aquatic-related grasses/herbs and are inferred to better reflect changes in the water availability of the study area and the isotopic compositions of lake water. However, the aquatic origin of these homologs should be ensured in downcore reconstructions, for instance, performing compound-specific carbon isotopic analysis. The use δD of C_{29} in the lake sediments (δD_{terr}) is interpreted as a robust terrestrial hydrology indicator. Despite the small number of plant species and different ε_{app} among modern plants, the integrated ε_{app} value of Lake Peixão's climatic sensor, determined from δD_{terr} ($\varepsilon_{C29/MAP} = -129 \pm 12‰$), is in line with the projected values of global compilation studies. Overall, this dataset establishes a baseline for interpreting the leaf wax biomarkers in the region and Lake Peixão sediments, which is a valuable archive to reconstruct regional past hydroclimate changes in the region.

Data availability statement

The original contributions presented in the study are included in the article/Supplementary Material, further inquiries can be directed to the corresponding authors.

Author contributions

RS collected the data. RS, ES, LC, and TR produced the data. RS wrote the manuscript. DO, AH, and AR contributed to improving the manuscript. All authors contributed to the discussion and interpretation of the data and provided comments and suggestions to the manuscript.

Funding

Acknowledgments

Conflict of interest

The authors declare that the research was conducted in the absence of any commercial or financial relationships that could be construed as a potential conflict of interest.

Publisher's note

All claims expressed in this article are solely those of the authors and do not necessarily represent those of their affiliated organizations, or those of the publisher, the editors and the reviewers. Any product that may be evaluated in this article, or claim that may be made by its manufacturer, is not guaranteed or endorsed by the publisher.

Supplementary material

The Supplementary Material for this article can be found online at: https://www.frontiersin.org/articles/10.3389/fenvs.2022.994377/full#supplementary-material

References

Abrantes, F., Rodrigues, T., Rufino, M., Salgueiro, E., Oliveira, D., Gomes, S., et al. (2017). The climate of the common era off the iberian Peninsula. *Clim. Past.* 13, 1901–1918. doi:10.5194/cp-13-1901-2017

Adrian, R., O'Reilly, C. M., Zagarese, H., Baines, S. B., Hessen, D. O., Keller, W., et al. (2009). Lakes as sentinels of climate change. *Limnol. Oceanogr.* 54, 2283–2297. doi:10.4319/lo.2009.54.6_part_2.2283

Allan, R. P., Hawkins, E., Bellouin, N., and Collins, B. (2021). "IPCC, 2021: Summary for policymakers," in *Climate change 2021: The physical science basis. Contribution of working group I to the sixth assessment report of the intergovernmental panel on climate change*. V. Masson-Delmotte, P. Zhai, A. Pirani, S. L. Connors, C. Péan, S. Berger, et al. (Cambridge University Press).

Baldini, L. M., Baldini, J. U. L., McDermott, F., Arias, P., Cueto, M., Fairchild, I. J., et al. (2019). North iberian temperature and rainfall seasonality over the younger dryas and holocene. *Quat. Sci. Rev.* 226, 105998. doi:10.1016/j.quascirev.2019.105998

Berke, M. A. (2018). "Reconstructing terrestrial paleoenvironments using sedimentary organic biomarkers BT - methods in paleoecology," in *Reconstructing cenozoic terrestrial environments and ecological communities*. Editors D. A. Croft, D. F. Su, and S. W. Simpson (Cham: Springer International Publishing), 121–149. doi:10.1007/978-3-319-94265-0_8

Boavida, M. J., and Gliwicz, Z. M. (1996). Limnological and biological characteristics of the alpine lakes of Portugal. *Limnetica* 12, 39–45. doi:10.23818/limn.12.11

Bowen, G. J., and Revenaugh, J. (2003). Interpolating the isotopic composition of modern meteoric precipitation. *Water Resour. Res.* 39, 1299. doi:10.1029/2003WR002086

Bray, E. E., and Evans, E. D. (1961). Distribution of n-paraffins as a clue to recognition of source beds. *Geochim. Cosmochim. Acta* 22, 2–15. doi:10.1016/0016-7037(61)90069-2

Bush, R. T., and McInerney, F. A. (2013). Leaf wax n-alkane distributions in and across modern plants: Implications for paleoecology and chemotaxonomy. *Geochim. Cosmochim. Acta* 117, 161–179. doi:10.1016/j.gca.2013.04.016

Carreira, P. M., Marques, J. M., Marques, J. E., Chaminé, H. I., Fonseca, P. E., Santos, F. M., et al. (2011). Defining the dynamics of groundwater in Serra da Estrela Mountain area, central Portugal: An isotopic and hydrogeochemical approach. *Hydrogeol. J.* 19, 117–131. doi:10.1007/s10040-010-0675-0

Carreira, P. M., Nunes, D., Valério, P., and Araújo, M. F. (2009). A 15-year record of seasonal variation in the isotopic composition of precipitation water over continental Portugal. *J. Radioanal. Nucl. Chem.* 281, 153–156. doi:10.1007/s10967-009-0064-0

Carvalho, A. M. M. (2013). *Hidrogeologia ambiental da região do Parque Natural da Serra da Estrela (setor de Seia - Torre - Covilhã): uma abordagem multidisciplinar*, 336.

Castañeda, I. S., and Schouten, S. (2011). A review of molecular organic proxies for examining modern and ancient lacustrine environments. *Quat. Sci. Rev.* 30, 2851–2891. doi:10.1016/j.quascirev.2011.07.009

Connor, S. E., van Leeuwen, J. F. N., van der Knaap, W. O., Pim)Akindola, R. B., Adeleye, M. A., et al. (2021). Pollen and plant diversity relationships in a Mediterranean montane area. *Veg. Hist. Archaeobot.* 30, 583–594. doi:10.1007/s00334-020-00811-0

Cortesi, N., Trigo, R. M., Gonzalez-Hidalgo, J. C., and Ramos, A. M. (2013). Modelling monthly precipitation with circulation weather types for a dense network of stations over Iberia. *Hydrol. Earth Syst. Sci.* 17, 665–678. doi:10.5194/hess-17-665-2013

Cranwell, P. A., Eglinton, G., and Robinson, N. (1987). Lipids of aquatic organisms as potential contributors to lacustrine sediments—II. *Org. Geochem.* 11, 513–527. doi:10.1016/0146-6380(87)90007-6

Curtin, L., Andrea, W. J. D., Balascio, N., Pugsley, G., Wet, G. De, and Bradley, R. (2019). Holocene and Last Interglacial climate of the Faroe Islands from sedimentary plant wax hydrogen and carbon isotopes. *Quat. Sci. Rev.* 223, 105930. doi:10.1016/j.quascirev.2019.105930

Dasgupta, B., Ajay, A., Prakash, P., and Sanyal, P. Understanding the disparity in n-alkane production among angiosperms and gymnosperms from the higher Himalayas: Inferences drawn from a Machine Learning approach. *Org. Geochem.* 171, 104463. doi:10.1016/J.ORGGEOCHEM.2022.104463

Diefendorf, A. F., Bickford, C. P., Schlanser, K. M., Freimuth, E. J., Hannon, J. S., Grossiord, C., et al. (2021). Plant wax and carbon isotope response to heat and drought in the conifer Juniperus monosperma. *Org. Geochem.* 153, 104197. doi:10.1016/j.orggeochem.2021.104197

Diefendorf, A., and Freimuth, E. (2017). Extracting the most from terrestrial plant-derived n-alkyl lipids and their carbon isotopes from the sedimentary record: A review. *Org. Geochem.* 103, 1–21. doi:10.1016/j.orggeochem.2016.10.016

Eglinton, G., and Hamilton, R. J. (1967). Leaf epicuticular waxes : The waxy outer surfaces of most plants display a wide diversity of fine structure and chemical constituents. *Sci. (80-.)* 156, 1322–1335. doi:10.1126/science.156.3780.1322

Evans, M. N., Tolwinski-Ward, S. E., Thompson, D. M., and Anchukaitis, K. J. (2013). Applications of proxy system modeling in high resolution paleoclimatology. *Quat. Sci. Rev.* 76, 16–28. doi:10.1016/j.quascirev.2013.05.024

Ferreira, L. M. M., Oliván, M., Celaya, R., Garcia, U., Rodrigues, M. A. M., and Osoro, K. (2007). The use of n-alkanes to estimate diet composition of ruminants grazing on species diverse plant communities - effect of feeding selectivity on diet composition estimates. *Livest. Sci.* 111, 114–123. doi:10.1016/j.livsci.2006.12.008

Ficken, K. J., Li, B., Swain, D. L., and Eglinton, G. (2000). An n-alkane proxy for the sedimentary input of submerged/floating freshwater aquatic macrophytes. *Org. Geochem.* 31, 745–749. doi:10.1016/S0146-6380(00)00081-4

Freeman, K. H., and Colarusso, L. A. (2001). Molecular and isotopic records of C4 grassland expansion in the late miocene. *Geochim. Cosmochim. Acta* 65, 1439–1454. doi:10.1016/S0016-7037(00)00573-1

Freimuth, E. J., Diefendorf, A. F., and Lowell, T. V. (2017). Hydrogen isotopes of n-alkanes and n-alkanoic acids as tracers of precipitation in a temperate forest and implications for paleorecords. *Geochim. Cosmochim. Acta* 206, 166–183. doi:10.1016/j.gca.2017.02.027

Gao, L., Edwards, E. J., Zeng, Y., and Huang, Y. (2014). Major evolutionary trends in hydrogen isotope fractionation of vascular plant leaf waxes. *PLoS One* 9, e112610. doi:10.1371/journal.pone.0112610

García-Alix, A., Camuera, J., Ramos-Román, M. J., Toney, J. L., Sachse, D., Schefuß, E., et al. (2021). Paleohydrological dynamics in the Western Mediterranean during the last glacial cycle. *Glob. Planet. Change* 202, 103527. doi:10.1016/j.gloplacha.2021.103527

Giménez, R., Bartolomé, M., Gázquez, F., Iglesias, M., and Moreno, A. (2021). Underlying climate controls in triple oxygen (16O, 17O, 18O) and hydrogen (1H, 2H) isotopes composition of rainfall (central pyrenees). *Front. Earth Sci.* 9, 1–16. doi:10.3389/feart.2021.633698

Hahn, A., Neumann, F. H., Miller, C., Finch, J., Frankland, T., Cawthra, H. C., et al. (2021). Mid-to late holocene climatic and anthropogenic influences in mpondoland, south Africa. *Quat. Sci. Rev.* 261, 106938. doi:10.1016/j.quascirev.2021.106938

Hammer, Ø., Harper, D., and Ryan, P. (2001). Past: Paleontological statistics software package for educaton and data anlysis. *Palaeontol. Electron.* 4, 1.

Hernández, A., Sáez, A., Santos, N. R., Rodrigues, T., Martin-Puertas, C., Gil-Romera, G., et al. (in review)). The timing of the deglaciation in the atlantic iberian mountains: Insights from the stratigraphical analysis on of a lake sediments sequence in Serra da Estrela (Portugal) (submitted). *Earth Surf. Process. Landforms.*

Hockun, K., Mollenhauer, G., Ling, S., Hefter, J., Ohlendorf, C., Zolitschka, B., et al. (2016). Using distributions and stable isotopes of n-alkanes to disentangle organic matter contributions to sediments of Laguna Potrok Aike, Argentina. *Org. Geochem.* 102, 110–119. doi:10.1016/j.orggeochem.2016.10.001

Hou, J., D'Andrea, W. J., MacDonald, D., and Huang, Y. (2007). Evidence for water use efficiency as an important factor in determining the δD values of tree leaf waxes. *Org. Geochem.* 38, 1251–1255. doi:10.1016/j.orggeochem.2007.03.011

Howard, S., McInerney, F. A., Caddy-Retalic, S., Hall, P. A., and Andrae, J. W. (2018). Modelling leaf wax n-alkane inputs to soils along a latitudinal transect across Australia. *Org. Geochem.* 121, 126–137. doi:10.1016/j.orggeochem.2018.03.013

Imfeld, A., Ouellet, A., Douglas, P. M. J., Kos, G., and Gélinas, Y. (2022). Molecular and stable isotope analysis (δ13C, δ2H) of sedimentary n-alkanes in the St. Lawrence Estuary and Gulf, Quebec, Canada: Importance of even numbered n-alkanes in coastal systems. *Org. Geochem.* 164, 104367. doi:10.1016/j.orggeochem.2022.104367

Jansen, J. (2011). *Managing Natura 2000 in a changing world the case of the Serra da Estrela.*

Jambrina-Enríquez, M., Sachse, D., and Valero-Garcés, B. L. (2016). A deglaciation and holocene biomarker-based reconstruction of climate and environmental variability in NW iberian Peninsula: The sanabria lake sequence. *J. Paleolimnol.* 56, 49–66. doi:10.1007/s10933-016-9890-6

Jiménez-moreno, G., García-alix, A., Hernández-corbalán, M. D., Anderson, R. S., and Delgado-huertas, A. (2013). Vegetation, fire, climate and human disturbance history in the southwestern Mediterranean area during the late Holocene. *Quat. Res.* 79, 110–122. doi:10.1016/j.yqres.2012.11.008

Leider, A., Hinrichs, K. U., Schefuß, E., and Versteegh, G. J. M. (2013). Distribution and stable isotopes of plant wax derived n-alkanes in lacustrine, fluvial and marine surface sediments along an Eastern Italian transect and their potential to reconstruct the hydrological cycle. *Geochim. Cosmochim. Acta* 117, 16–32. doi:10.1016/j.gca.2013.04.018

Li, Z., Sun, Y., and Nie, X. (2020). Biomarkers as a soil organic carbon tracer of sediment: Recent advances and challenges. *Earth. Sci. Rev.* 208, 103277. doi:10.1016/j.earscirev.2020.103277

Liu, H., and Liu, W. (2019). Hydrogen isotope fractionation variations of n-alkanes and fatty acids in algae and submerged plants from Tibetan Plateau lakes: Implications for palaeoclimatic reconstruction. *Sci. Total Environ.* 695, 133925. doi:10.1016/j.scitotenv.2019.133925

Liu, J., An, Z., and Liu, H. (2018). Leaf wax n-alkane distributions across plant types in the central Chinese Loess Plateau. *Org. Geochem.* 125, 260–269. doi:10.1016/j.orggeochem.2018.09.006

Liu, J., and An, Z. (2019). Variations in hydrogen isotopic fractionation in higher plants and sediments across different latitudes: Implications for paleohydrological reconstruction. *Sci. Total Environ.* 650, 470–478. doi:10.1016/j.scitotenv.2018.09.047

Loidi, J., Biurrun, I., Campos, J. A., García-Mijangos, I., and Herrera, M. (2007). A survey of heath vegetation of the iberian Peninsula and northern Morocco: A biogeographic and bioclimatic approach. *phyto.* 37, 341–370. doi:10.1127/0340-269X/2007/0037-0341

López-Días, V., Blanco, C. G., Bechtel, A., Püttmann, W., and Borrego, A. G. (2013). Different source of n-alkanes and n-alkan-2-ones in a 6000cal. yr BP Sphagnum-rich temperate peat bog (Roñanzas, N Spain). *Org. Geochem.* 57, 7–10. doi:10.1016/j.orggeochem.2013.01.006

Marzi, R., Torkelson, B. E., and Olson, R. K. (1993). A revised carbon preference index. *Org. Geochem.* 20, 1303–1306. doi:10.1016/0146-6380(93)90016-5

McFarlin, J. M., Axford, Y., Masterson, A. L., and Osburn, M. R. (2019). Calibration of modern sedimentary δ2H plant wax-water relationships in Greenland lakes. *Quat. Sci. Rev.* 225, 105978. doi:10.1016/j.quascirev.2019.105978

Mora, C. (2010). A synthetic map of the climatopes of the Serra da Estrela (Portugal). *J. Maps* 6, 591–608. doi:10.4113/jom.2010.1112

Oliveira, A., and Lima, A. (2010). Spatial variability in the stable isotopes of modern precipitation in the northwest of Iberia. *Isot. Environ. Health Stud.* 46, 13–26. doi:10.1080/10256010903388154

Ortiz, J. E., Borrego, Á. G., Gallego, J. L. R., Sánchez-Palencia, Y., Urbanczyk, J., Torres, T., et al. (2016). Biomarkers and inorganic proxies in the paleoenvironmental reconstruction of mires: The importance of landscape in Las Conchas (Asturias, Northern Spain). *Org. Geochem.* 95, 41–54. doi:10.1016/j.orggeochem.2016.02.009

Ortiz, J. E., Díaz-Bautista, A., Aldasoro, J. J., Torres, T., Gallego, J. L. R., Moreno, L., et al. (2011). N-Alkan-2-ones in peat-forming plants from the Roñanzas ombrotrophic bog (Asturias, northern Spain). *Org. Geochem.* 42, 586–592. doi:10.1016/j.orggeochem.2011.04.009

Ortiz, J. E., Torres, T., Delgado, A., Llamas, J. F., Soler, V., Valle, M., et al. (2010). Palaeoenvironmental changes in the Padul Basin (Granada, Spain) over the last 1Ma based on the biomarker content. *Palaeogeogr. Palaeoclimatol. Palaeoecol.* 298, 286–299. doi:10.1016/j.palaeo.2010.10.003

Ortiz, J. E., Torres, T., Delgado, A., Valle, M., Soler, V., Araujo, R., et al. (2021). Bulk and compound-specific δ13C and n-alkane indices in a palustrine intermontane record for assessing environmental changes over the past 320 ka: The padul basin (southwestern mediterranean realm). *J. Iber. Geol.* 47, 625–639. doi:10.1007/s41513-021-00175-y

Pancost, R. D., and Boot, C. S. (2004). The palaeoclimatic utility of terrestrial biomarkers in marine sediments. *Mar. Chem.* 92, 239–261. doi:10.1016/j.marchem.2004.06.029

Pérez Latorre, A. V., and Cabezudo, B. (2002). Use of monocharacteristic growth forms and phenological phases to describe and differentiate plant communities in Mediterranean-type ecosystems. *Plant Ecol.* 161, 231–249. doi:10.1023/A:1020327522487

Peters, K. E., Peters, K. E., Walters, C. C., and Moldowan, J. M. (2005). *The biomarker guide.* Cambridge University Press.

Post-Beittenmiller, D. (1996). Biochemistry and molecular biology of wax production in plants. *Annu. Rev. Plant Physiol. Plant Mol. Biol.* 47, 405–430. doi:10.1146/annurev.arplant.47.1.405

Poynter, J. G. (1989). *Molecular stratigraphy: The recognition of palaeoclimatic signals in organic geochemical data.* Bristol: School of Chemistry, University of Bristol. PhD Thesis.

Ribeiro, A., Kullberg, M. C., Kullberg, J. C., Manuppella, G., and Phipps, S. (1990). A review of Alpine tectonics in Portugal: Foreland detachment in basement and cover rocks. *Tectonophysics* 184, 357–366. doi:10.1016/0040-1951(90)90448-H

Rommerskirchen, F., Eglinton, G., Dupont, L., and Rullkötter, J. (2006). Glacial/interglacial changes in southern Africa: Compoundspecific δ13C land plant biomarker and pollen records from southeast Atlantic continental margin sediments. *Geochem. Geophys. Geosyst.* 7. doi:10.1029/2005GC001223

Sachse, D., Billault, I., Bowen, G. J., Chikaraishi, Y., Dawson, T. E., Feakins, S. J., et al. (2012). Molecular paleohydrology: Interpreting the hydrogen-isotopic composition of lipid biomarkers from photosynthesizing organisms. *Annu. Rev. Earth Planet. Sci.* 40, 221–249. doi:10.1146/annurev-earth-042711-105535

Sánchez-López, G., Hernández, A., Pla-Rabes, S., Trigo, R. M., Toro, M., Granados, I., et al. (2016). Climate reconstruction for the last two millennia in central Iberia: The role of east atlantic (EA), North Atlantic oscillation (NAO) and their interplay over the iberian Peninsula. *Quat. Sci. Rev.* 149, 135–150. doi:10.1016/j.quascirev.2016.07.021

Schäfer, I. K., Bliedtner, M., Wolf, D., Faust, D., and Zech, R. (2016a). Evidence for humid conditions during the last glacial from leaf wax patterns in the loess-paleosol sequence El Paraíso, Central Spain. *Quat. Int.* 407, 64–73. doi:10.1016/j.quaint.2016.01.061

Schäfer, I. K., Lanny, V., Franke, J., Eglinton, T. I., Zech, M., Vysloužilová, B., et al. (2016b). Leaf waxes in litter and topsoils along a European transect. *Soil* 2, 551–564. doi:10.5194/soil-2-551-2016

Schefuß, E., Ratmeyer, V., Stuut, J. B. W., Jansen, J. H. F., and Sinninghe Damsté, J. S. (2003). Carbon isotope analyses of n-alkanes in dust from the lower atmosphere over the central eastern Atlantic. *Geochim. Cosmochim. Acta* 67, 1757–1767. doi:10.1016/S0016-7037(02)01414-X

Schirrmacher, J., Andersen, N., Schneider, R. R., and Weinelt, M. (2020). Fossil leaf wax hydrogen isotopes reveal variability of Atlantic and Mediterranean climate forcing on the southeast Iberian Peninsula between 6000 to 3000 cal. BP. *PLoS One* 15, 1–19. doi:10.1371/journal.pone.0243662

Shepherd, T., and Griffiths, D. W. (2006). The effects of stress on plant cuticular waxes. *New Phytol.* 171, 469–499. doi:10.1111/j.1469-8137.2006.01826.x

Stout, S. A. (2020). Leaf wax n-alkanes in leaves, litter, and surface soil in a low diversity, temperate deciduous angiosperm forest, Central Missouri, USA. *Chem. Ecol.* 0, 810–826. doi:10.1080/02757540.2020.1789118

Taylor, A. K., Benedetti, M. M., Haws, J. A., and Lane, C. S. (2018). Mid-holocene iberian hydroclimate variability and paleoenvironmental change: Molecular and isotopic insights from praia rei cortiço, Portugal. *J. Quat. Sci.* 33, 79–92. doi:10.1002/jqs.3000

Thatcher, D. L., Wanamaker, A. D., Denniston, R. F., Asmerom, Y., Polyak, V. J., Fullick, D., et al. (2020). Hydroclimate variability from Western Iberia (Portugal) during the Holocene: Insights from a composite stalagmite isotope record. *Holocene* 30, 966–981. doi:10.1177/0959683620908648

Thomas, C. L., Jansen, B., Van Loon, E. E., and Wiesenberg, G. L. B. (2021). Transformation of <i&gt;n&lt;/i&gt;-alkanes from plant to soil: A review. *SOIL* 7, 785–809. doi:10.5194/soil-7-785-2021

Thomas, P. A., El-Barghathi, M., and Polwart, A. (2007). Biological flora of the British isles: Juniperus communis L. *J. Ecol.* 95, 1404–1440. doi:10.1111/j.1365-2745.2007.01308.x

Toney, J. L., García-Alix, A., Jiménez-Moreno, G., Anderson, R. S., Moossen, H., and Seki, O. (2020). New insights into Holocene hydrology and temperature from lipid biomarkers in Western Mediterranean alpine wetlands. *Quat. Sci. Rev.* 240, 106395. doi:10.1016/j.quascirev.2020.106395

Toro, M., Granados, I., Robles, S., and Montes, C. (2006). High mountain lakes of the central range (iberian Peninsula): Regional limnology & environmental changes. *Limnetica* 25, 217–252. doi:10.23818/limn.25.17

Vieira, G. (2008). Combined numerical and geomorphological reconstruction of the Serra da Estrela plateau icefield, Portugal. *Geomorphology* 97, 190–207. doi:10.1016/j.geomorph.2007.02.042

Vieira, G. (2004). *Geomorfologia dos planaltos E altos vales da Serra da Estrela ambientes frios do plistocénico superior E dinâmica actual*. Lisbon: University of Lisbon. PhD Thesis.

Vieira, G., Jansen, J., and Ferreira, N. (2005). *Environmental setting of the Serra da Estrela, Portugal a short-note*. IALE UK: Landsc. Ecol. Ser.

Wang, J., Axia, E., Xu, Y., Wang, G., Zhou, L., Jia, Y., et al. (2018). Temperature effect on abundance and distribution of leaf wax n-alkanes across a temperature gradient along the 400 mm isohyet in China. *Org. Geochem.* 120, 31–41. doi:10.1016/j.orggeochem.2018.03.009

Xie, M., Sun, Q., Dong, H., Liu, S., Shang, W., Ling, Y., et al. (2020). n-Alkanes and compound carbon isotope records from Lake Yiheshariwusu in the Hulun Buir sandy land, northeastern China. *Holocene* 30, 1451–1461. doi:10.1177/0959683620932968

Yang, H., Liu, W., Leng, Q., Hren, M. T., and Pagani, M. (2011). Variation in n-alkane δD values from terrestrial plants at high latitude: Implications for paleoclimate reconstruction. *Org. Geochem.* 42, 283–288. doi:10.1016/j.orggeochem.2011.01.006

Zech, M., Buggle, B., Leiber, K., Marković, S., Glaser, B., Hambach, U., et al. (2010). Reconstructing Quaternary vegetation history in the Carpathian Basin, SE-Europe, using n-alkane biomarkers as molecular fossils: Problems and possible solutions, potential and limitations. *E&amp;G Quat. Sci. J.* 58, 148–155. doi:10.3285/eg.58.2.03